Simulative determination of kinetic coefficients for nucleation rates

P. Schaaf, B. Senger, J.-C. Voegel, R. K. Bowles, and H. Reiss

Citation: The Journal of Chemical Physics **114**, 8091 (2001); doi: 10.1063/1.1364640
View online: http://dx.doi.org/10.1063/1.1364640
View Table of Contents: http://scitation.aip.org/content/aip/journal/jcp/114/18?ver=pdfcov
Published by the AIP Publishing

Simulative determination of kinetic coefficients for nucleation rates

P. Schaaf[a)]
Institut Charles Sadron, CNRS-ULP, 6, rue Boussingault, 67083 Strasbourg Cedex, France

B. Senger and J.-C. Voegel
Institut National de la Santé et de la Recherche Médicale. Unité 424, Fédération de Recherches ''Odontologie,'' Université Louis Pasteur, 11, rue Humann, 67085 Strasbourg Cedex, France

R. K. Bowles and H. Reiss
Department of Chemistry and Biochemistry, University of California, 405 Hilgard Avenue, Los Angeles, California 90095-1569

(Received 22 November 2000; accepted 20 February 2001)

Nucleation kinetics can be formulated generally and rigorously as a set of master equations that govern the time evolution of the cluster distribution that underlies the observable rate process. However, this general formulation is only useful if the magnitudes of the coefficients that describe the loss and gain (evaporation and condensation) of molecules by a cluster are quantitatively known. Moreover, these coefficients can refer to multiple losses and gains of molecules (several molecules in a single step). In order to measure these coefficients accurately and efficiently, we have devised a molecular dynamics (MD) simulation that follows the development and equilibration of a single cluster in a small container (volume) that involves only a small number of molecules (in our case 216). There is evidence that such a system can provide a reliable picture of the behavior of a cluster in a larger system. This approach has been applied to supersaturated argon vapor at 85 K. In particular, we have been able to study the fluctuation in the size of the ''equilibrium'' cluster that develops in the small volume and, from these observations, to determine the evaporation and condensation coefficients. Besides yielding the values of these coefficients, the study has allowed us to establish several points, including the validity of detailed balance within the simulation, the importance of multimolecular losses and gains of molecules, and the intrinsic nature (nonimportance of the surrounding vapor) of the evaporation coefficients. Also, it is shown that the clusters disappear by a first order decay law, thus establishing the relevance of the linear form of the set of master equations that can be used to describe the nucleation process. It is also established, by our first estimates of the condensation coefficients, that they are an order of magnitude larger than those predicted by the simple molecular kinetic theory used in classical nucleation theory (CNT), suggesting the effects of the diffuse outer layers of the actual physical cluster and the role of the cluster's attractive potential. In addition, we have performed an analysis, involving the statistics of correlation, that strongly supports the idea that multimolecule losses and gains experienced by a cluster are chiefly due to the departure and arrival of smaller ''clusters.'' Finally, we have modeled the nucleation process in the small system, using CNT, and have found that in many respects CNT provides a good account of the phenomena observed by means of MD. Because of the ''intrinsic nature'' of the evaporation coefficient, it is possible to perform the simulations at quite high levels of supersaturation, thereby accelerating the approach to equilibrium, and requiring less computer capacity. The evaporation coefficient of the ''equilibrium cluster'' that forms the object of our measurement is insensitive to the level of supersaturation of the surrounding medium. The condensation coefficient can then be determined by an application of the principle of detailed balance, once the equilibrium distribution of clusters in a particular nucleating system is known. Thus apart from our focus on evaporation and condensation coefficients, the small system appears to be useful in the modeling of nucleation phenomena in general. [DOI: 10.1063/1.1364640]

I. ORIGIN OF THE PROBLEM

As is well known, nucleation theory can be viewed as composed of two distinct but not entirely separable parts. These are focused, respectively, on the *thermodynamic* and *kinetic* aspects of the phenomenon. Over the years, impressive progress has been made in the development of the thermodynamic aspects of nucleation theory, and this has included theory at the molecular level aided by simulation.[1–15] In contrast, advances in the kinetic arena, prerequisite to the development of an accurate theory of rate, have been few and far between. Recently, however, Frenkel and ten Wolde

[a)]Author to whom correspondence should be addressed. Electronic mail: schaaf@ics.u-strasbg.fr

and their co-workers[7] have made an important advance in which the nucleation rate is calculated making use of a constrained equilibrium distribution of clusters in the neighborhood of the nucleus together with the evaluation of the response coefficients of the system determined through the application of linear response theory in the mode applied to chemical reaction rates.[16–18] Of course this presumes the applicability of linear response theory, but there are strong reasons for believing that it is applicable to the nucleation problem. Like other molecular approaches, the method of Frenkel and ten Wolde, requires the assistance of computer simulation.

It is, of course, desirable to complement the linear response approach with other molecular theories of rate that may or may not require some simulation. Quantitative agreement between linear response and another of these approaches would reinforce the validities of both. Toward this end, we have developed an alternative approach based on the following set of master equations:

$$J(n\rightarrow n')=\beta(n\rightarrow n')N(n)-\gamma(n'\rightarrow n)N(n'), \quad n'>n, \tag{1a}$$

$$\frac{dN(n)}{dt}=\sum_{n'=1}^{n-1} J(n'\rightarrow n)-\sum_{n'=n+1}^{\infty} J(n\rightarrow n'), \tag{1b}$$

where $N(n)$ represents the number of n clusters present in the system at a given time t, $\beta(a\rightarrow b)$ and $\gamma(a\rightarrow b)$ correspond, respectively, to the condensation and evaporation coefficients for a transition from an a to a b cluster, and $J(a\rightarrow b)$ is the net flux from a to b clusters. In order to use and solve this set of master equations, the kinetic coefficients must be known. Moreover, a precise definition of the clusters to which $N(n)$ refers is required. This definition must allow the identification of clusters in a nonredundant manner,[12,19,20] and also make it possible to take the translational free energy of the cluster into account,[21] especially under equilibrium conditions. This problem has been addressed extensively during the last few years,[7,12] and one of the most successful definitions is that of the so-called Stillinger cluster,[22] in which a molecule is part of a cluster if it is closer than some prescribed (connectivity) distance to at least one other molecule of the cluster, while it is part of the surrounding medium if it fails this test. The Stillinger cluster possesses all of the desirable properties mentioned above, but it still remains to be proved that it is capable of accounting accurately for observed nucleation rates.

Still, in this paper, we will attempt to evaluate the condensation and evaporation coefficients β and γ for a Stillinger cluster. We will attempt to accomplish this, accurately, with the aid of molecular dynamics (MD) simulations, involving small systems and small numbers of molecules ($\sim$200). The focus on the use of small systems in the study of nucleation phenomena occurring in systems, large enough to be in the thermodynamic limit, is not original with us,[7,8,10,11,13] but up to now we mainly concentrated on equilibrium aspects whereas here we concentrate on the evaluation of the kinetic coefficients.

Although the β's and γ's that we evaluate are supposed to be those that apply to a macroscopic system, the actual simulations involve a small system. The aim of the paper is thus twofold. We first develop several new aspects of classical nucleation theory (CNT),[23] that apply specifically to a small system. These aspects should be very valuable for future simulations. We then concentrate on the determination of the kinetic parameters characterizing the clusters entering in the nucleation rate theory.

II. CLASSICAL NUCLEATION THEORY FOR SMALL *N*, *V*, *T* SYSTEMS

Consider a cubic container of volume V in which there are N molecules at temperature T. We will simply ignore special behavior that occurs at the walls of the container. We do this to prepare our perspective for the problem of primary interest, namely the MD simulation of cluster formation in a system of similar volume, but subject to periodic boundary conditions that, in effect, remove the influence of the walls.

On a purely qualitative basis, what should we expect in such a small system that is qualitatively, but dramatically, different from our expectation in a large system? Consider a situation in which the N molecules initially constitute a vapor that is supersaturated with respect to condensation, i.e., N is sufficiently large for a given volume V. Condensation will occur via a clustering process involving a free energy barrier where the cluster at the top of the barrier is the nucleus. Ultimately (at least in CNT), the nucleus will grow into a single ''drop,'' surrounded by vapor, which (at equilibrium) can fluctuate in size and wander throughout V. The drop cannot be arbitrarily large since N is finite, and more importantly, because it must satisfy the Kelvin relation[24] with respect to the surrounding vapor. From the point of view of the free energy of the system, the drop corresponds to a free energy minimum whereas the cluster at the top of the barrier (nucleus) corresponds to a free energy maximum.

The formation of an equilibrium drop in a finite volume is a well known phenomenon.[3–6,25] It has been observed in several simulations[4,5] and in approximate analytical calculations[6] based on intermolecular potentials, and it has been predicted by thermodynamic theory.[25] There is a critical value of V, for given N, beyond which a stable equilibrium drop cannot be formed.[25]

However, the radial density profile derived from this drop has been interpreted in a number of ways. For example, it is possible to consider the profile within the drop itself,[11] or to consider the profile that results from considering the local density as an average of the density produced by the wandering drop. The former point of view is taken by Kusaka *et al.*[11] in recent studies on the formation and identification of clusters, whereas the latter picture is what results from density functional (DF) studies,[5] simulations due Abraham and co-workers,[2] as well as from the ''modified liquid drop theory'' of Weakliem and Reiss.[6] The profile appearing in the latter picture is what derives from a strict thermodynamic approach, but the former picture is equally valid, as another face of the same coin, but can only be obtained with the aid of the ''mathematical microscopy'' available in computer simulation.

In contrast to the behavior described above, in an initially macroscopic system, the resulting drop (or drops)

grows until the pressure of the remaining vapor equals the vapor pressure of the bulk liquid in question, i.e., until it or they satisfy the Kelvin relation for a drop with infinite radius of curvature or until the system is just saturated. In principle, given enough time, an Ostwald ripening process[26] should occur until only a single monolithic drop remains, but as a practical matter this never occurs.

In a simulation based on the intermolecular potential a single equilibrium cluster will also form in the small system. We shall make use of this equilibrium cluster in the evaluation of the desired evaporation coefficients γ, but first we appeal to CNT in order to demonstrate the above in a more palpable manner.

It is convenient to begin with the formula that expresses the probability of finding, in the system, *at least* one cluster consisting of n molecules. Quite generally, and not restricted to CNT, this is

$$P(n)=\frac{Q_n}{Q_S}, \tag{2}$$

where Q_n is the canonical ensemble partition function of the system constrained to have at least one cluster of size n and Q_S is the partition function of the unconstrained system. When n is large the probability of finding more than one n cluster in the small system is vanishingly small, so that $P(n)$ is essentially the probability of finding *exactly* one n cluster in the system. Then one can write

$$Q_S=Q_{n<n_0}+\sum_{i=n_0}^{N} Q_i, \tag{3}$$

where $Q_{n<n_0}$ represents the partition function of the system when it is constrained to contain only clusters of size smaller than n_0, and n_0 is such that when an n cluster ($n>n_0$) is present the probability of another n' cluster ($n'>n_0$) being present is vanishingly small.

We now evaluate Q_n within the special framework of CNT where an n cluster is modeled as a spherical liquid drop having a uniform density and a surface tension equal to the respective quantities in the bulk liquid, as well as a sharp interface with the surrounding vapor. Then the Helmholtz free energy of this drop, approximated as incompressible, is[27]

$$F_d(n)=n\mu_{\mathrm{liq}}+\sigma a_n-Pv_n, \tag{4}$$

where μ_{liq} is the chemical potential of a molecule in the bulk liquid at the pressure P outside of the drop, σ is the surface tension of the liquid, while a_n and v_n are, respectively, the area and volume of the drop. Note that $v_n=nv$ where v is the volume per molecule in the bulk liquid. The nature of the CNT model is such that the position of the drop is determined by the center of the sphere bounded by its surface, and not by its center of mass. Thus the partition function of the drop, fixed at a particular position within V, is prescribed by

$$q_n^f=\exp[-F_d(n)/kT], \tag{5}$$

where k is the Boltzmann constant. The $N-n$ molecules that remain in the volume $V-v_n$ belong to the surrounding gas or vapor. The cluster is considered to be decoupled from the surrounding gas (coupling free energy is assumed to be included in surface free energy density, i.e., in the surface tension σ). Then the partition function of the full system, cluster and gas, with the cluster fixed at a particular position, is given by

$$Q_n^0=Q_{N-n}^{(g)}(V-v_n)\exp[-(n\mu_{\mathrm{liq}}+\sigma a_n-Pv_n)/kT], \tag{6}$$

where $Q_{N-n}^{(g)}(V-v_n)$ is the partition function of a gas composed of $N-n$ molecules in the volume $V-v_n$. If the drop is approximated as incompressible, the chemical potential $\mu_{\mathrm{liq}}(P)$ is related to the chemical potential $\mu_{\mathrm{liq}}(P_e)$ at the saturation pressure P_e by

$$\mu_{\mathrm{liq}}(P)=\mu_{\mathrm{liq}}(P_e)+v(P-P_e)=\mu_{\mathrm{vap}}(P_e)+v(P-P_e), \tag{7}$$

where $\mu_{\mathrm{vap}}(P_e)$ is the chemical potential of the vapor in equilibrium, at the saturation pressure P_e, with bulk liquid, and is therefore equal to $\mu_{\mathrm{liq}}(P_e)$. Substitution of Eq. (7) into Eq. (6) yields

$$Q_n^0=Q_{N-n}^{(g)}(V-v_n)\exp\{-[n\mu_{\mathrm{vap}}(P_e)+\sigma a_n-P_e v_n]/kT\}. \tag{8}$$

In essence, Eq. (8) corresponds to the original CNT in which the effect of the multiple possible locations for the drop (cluster) anywhere within the volume V was not taken into account. In simple terms, the translational degrees of freedom of the cluster were not addressed. This omission, together with attempts to repair it, led to disagreement and problems like the ''replacement free energy'' controversy.[18] However, recently, agreement seems to have been reached concerning the best way to introduce translation into CNT.[19] This adjustment leads a modified partition function given by

$$Q_n=\frac{V}{\theta_n}Q_n^0, \tag{9}$$

where θ_n is a characteristic volume scale that defines the length through which the cluster has to be moved before the new configuration can be counted as a new physical state of the system. In phase space the fundamental length is Planck's constant, but after momenta have been integrated away, and we are left with the cluster in coordinate space and the special properties of the CNT model are considered, it turns out[19] that θ_n can be approximated as

$$\theta_n=\frac{kT}{\Pi_n+P}, \tag{10}$$

where P is the pressure of the surrounding vapor and

$$\Pi_n=kT\frac{\partial \ln q_n^f}{\partial v_n}. \tag{11}$$

It is also possible to show[19] that Π_n can be approximated as

$$\Pi_n=\sqrt{\frac{kT}{\kappa v_n}}, \tag{12}$$

where κ is the isothermal compressibility of the liquid drop. Usually κ is so small that $\Pi_n \gg P$ so that θ_n can be reduced to

$$\theta_n \approx \frac{kT}{\Pi_n} = \sqrt{kT\kappa v_n}. \tag{13}$$

It is interesting to note that θ_n prescribed by Eq. (13) is the volume of the ''breathing fluctuation'' (or the volume fluctuation) of the drop. The fact that the characteristic volume scale corresponds to the volume fluctuation is physically reasonable; it simply means that the drop cannot be located more accurately than within its volume of fluctuation so that the system cannot realize a new physical state until the drop has been displaced by a distance of the order of the cube root of the volume of fluctuation.

Substitution of Eq. (13) into Eq. (9) yields

$$Q_n = \frac{V}{\sqrt{kT\kappa v_n}} Q_n^0 \tag{14}$$

and assuming the vapor to be ideal, so that $Q_{N-n}^{(g)}(V-v_n)$ in Eq. (8) is the partition function of an ideal gas, we arrive at

$$Q_n = \frac{(V-v_n)^{N-n}}{(N-n)!(\Lambda^3)^{N-n}} \frac{V}{\sqrt{kT\kappa v_n}} \times \exp\{-[n\mu_{\text{vap}}(P_e) + \sigma a_n - P_e v_n]/kT\}, \tag{15}$$

where Λ is the thermal de Broglie wavelength of a molecule. Substitution of Eq. (3) into Eq. (2) gives

$$P(n) = \frac{Q_n}{Q_{n<n_0} + \Sigma_{i=n_0}^{N} Q_i}. \tag{16}$$

Continuing to assume that the vapor behaves as an ideal gas, we can write

$$\mu_{\text{vap}}(P_e) = kT \ln\left(\frac{\Lambda^3 P_e}{kT}\right) \tag{17}$$

which can be used in Eq. (15).

The denominator in Eq. (16) is independent of n, so that the extrema of $P(n)$ coincide with the extrema of Q_n whose functional dependence on n is fully specified by Eq. (15), when it is realized that $a_n = 4\pi(3vn/4\pi)^{2/3}$ and $P = (N-n)kT/(V-nv)$. Then the equation $(\partial \ln Q_n/\partial n)_{N,V,T} = 0$ can be expressed as

$$\ln\left(\frac{P}{P_e}\right) - \frac{1}{2n} + \frac{1}{2(N-n)} - \frac{8\pi\sigma}{3kT}\left(\frac{3v}{4\pi}\right)^{2/3} n^{-1/3} - \frac{v}{kT}(P-P_e) = 0. \tag{18}$$

Extrema of $P(n)$ are then obtained as the roots of this equation.

The third term in Eq. (18) vanishes in the thermodynamic limit, $N\to\infty$, $V\to\infty$, $N/V\to$constant, the second term comes from the translational effects that we have included in Q_n in Eq. (15), and the last term is usually neglected in CNT. Since translation is not included in CNT, and the usual system is in the thermodynamic limit, the neglect of the second, third, and last term in Eq. (18) should result in the conventional expression for n^*, the size of the nucleus in conventional CNT. Comparison with the conventional expression shows that this is indeed the case.

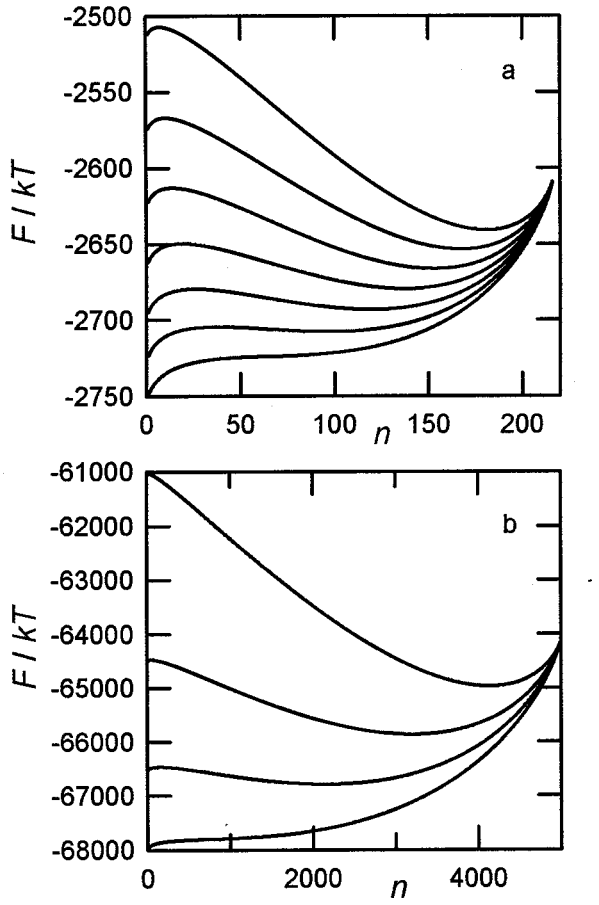

FIG. 1. Helmholtz free energy F of clusters, according to Eq. (15) and $F/kT = -\ln Q_n$ as a function of size n; (a) $N=216$ and container volumes $V/r_0^3 = 6000,\ 8000, \ldots, 18\,000$ (from top to bottom), (b) $N=5000$ and $V/r_0^3 = 2.5,\ 5,\ 7.5$, and 10×10^5 (from top to bottom). $T=85$ K, surface tension $\sigma = 13.2$ mJ m^{-2}, compressibility $\kappa = 10^{-9}$ Pa^{-1}.

We can now examine whether Eq. (18) confirms the scenario, for a small system, discussed qualitatively at the beginning of this section. Begin with Figs. 1(a) and 1(b) in which the free energy $F = -kT \ln Q_n$ (in fact F/kT) for an argon system, obtained using Eq. (15), is plotted as a function of n for different values of V/r_0^3 at fixed N, where r_0 is the length scale for the Lennard-Jones potential and is defined in Eq. (22) below. The figure shows that Eq. (18) possesses either two or no roots. When there are roots, the one at smaller n corresponds to a relative maximum that marks the top of a free energy barrier so that the root is $n=n^*$, the size of the nucleus. The larger root corresponds to a free energy minimum, and therefore to the stable equilibrium drop (cluster) described at the beginning of this section. Both roots disappear as V is increased, i.e., as the overall density, or the initial supersaturation, of the system is reduced below the critical value beyond which the equilibrium state of the system consists of a uniform vapor. Thus far, the qualitative scenario is confirmed.

Figure 2, again for argon, contains plots of the critical nucleus size n^*, of $S(n^*)$ the supersaturation that remains when the nucleus is formed, and of the barrier height, $\Delta F = F(n^*) - F(1)$, when it is defined (i.e., as long as n^* exists). The supersaturation is defined by the pressure ratio

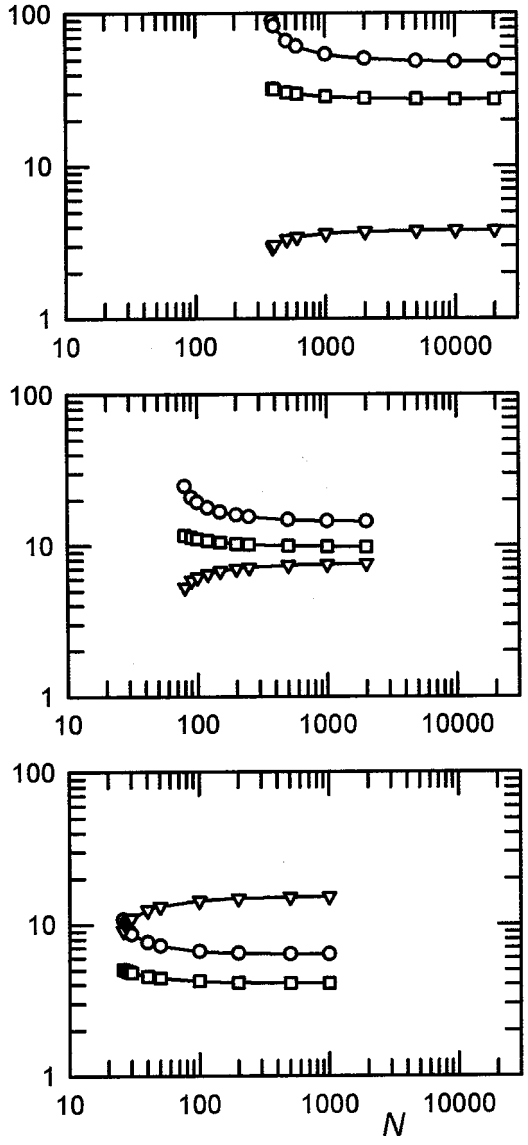

FIG. 2. Nucleus size n^* (circles), corresponding supersaturation $S(n^*)$ (triangles), and free energy barrier height $\Delta F/kT=[F(n^*)-F(1)]/kT$ (squares) as functions of the total number of atoms N for three values of the density N/V (determining together with $T=85$ K the initial supersaturation S_{init}). Top: $N/V=10^{-2}/r_0^3$ ($S_{\text{init}}=3.82$), middle: $N/V=2\times10^{-2}/r_0^3$ ($S_{\text{init}}=7.64$), bottom: $N/V=4\times10^{-2}/r_0^3$ ($S_{\text{init}}=15.28$). Vapor is assumed to behave ideally. Other parameters are the same as in Fig. 1.

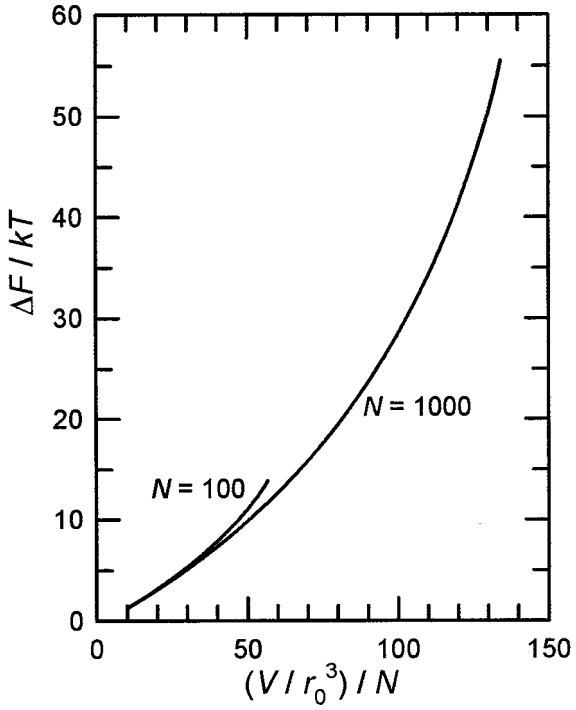

FIG. 3. Free energy barrier $\Delta F/kT=[F(n^*)-F(1)]/kT$, according to CNT adapted to small systems, as a function of reciprocal density. Curves for $N=100$ and $N=1000$ are plotted. F is obtained from Eq. (15). Parameters are those of Fig. 1.

$P(n^*)/P_0$, with $P(n^*)=(N-n^*)kT/(V-n^*v)$ if the vapor behaves as an ideal gas, and $P_0=133.32\times10^{6.9605-6826\times0.052\,23/T}$.[28] These quantities are plotted versus N for different values of N/V or, equivalently, different initial values of supersaturation S_{init}. We see that, for a given S_{init}, a critical value of N is required in order for a barrier to exist (and not merely a monotonically increasing free energy, as a function of n) and for a nucleation process to be observed. Furthermore, the height of the barrier increases as N decreases at fixed V until the barrier gives way to a monotone increasing free energy. Similarly, the barrier height increases with increasing V at fixed N, i.e., with decreasing initial supersaturation. However, as is illustrated in Fig. 3, the ratio N/V does not uniquely determine ΔF, except at high initial vapor densities (or $V/N\to0$). It is also worth noting that the larger the value of N, the smaller is the initial vapor density, or the initial supersaturation, that still gives rise to a barrier, and hence to nucleation.

Not all of the quantitative results discussed in the preceding paragraph were mentioned in the qualitative scenario described at the beginning of this section, but none of them contradict that scenario, and the rather detailed picture of the behavioral features of nucleation in a small system that they provide should be of considerable value in the design and interpretation of MD studies of nucleation in small systems, such as the studies reported in the remainder of this paper. For example, at $N/V=10^{-2}r_0^{-3}$ and $S_{\text{init}}=3.82$, the supersaturation at n^*, i.e., $S(n^*)$, becomes independent of N for $N\approx350$. This suggests that in a molecular simulation with $N/V=10^{-2}r_0^{-3}$, one should choose N to exceed 350.

In closing this section, it is appropriate to note that, in Sec. V A, the size distribution of the equilibrium cluster obtained using Eqs. (15) and (16), i.e., the fluctuation of its size, will be compared with the distributions obtained by means of MD. Reasonably good agreement is found between this result of CNT and the corresponding result of MD.

III. SOME KINETIC CONSIDERATIONS

Consider the time evolution of an ensemble of N_T small systems such as the one that we have been discussing. This evolution can be described by a set of master equations similar to Eq. (1) in which, now, $N(n,t)$ represents the number of small systems in the ensemble that, at time t, contain at least one n cluster. Developing the rate theory along exactly the same lines as CNT and using the same approximations, the steady state nucleation rate is expressed as

$$J=\frac{1}{N_T}\left\{\sum_{n=1}^{n_m}\left[\beta(n,n+1)N_e(n)\right]^{-1}\right\}^{-1}, \tag{19}$$

where n_m is a number larger than the nucleus size n^*, but smaller than the size of the equilibrium cluster in the small system. In the case of the ensemble, the nucleation rate J is the inverse of the mean time required for the formation of the equilibrium cluster in one of the small systems. $N_e(n)$ is the number of systems, in constrained equilibrium (no cluster larger than n_m) containing at least one n cluster. Thus

$$N_e(n)=N_T Q_n \Big/ \sum_{i=1}^{n_m} Q_i\,. \tag{20}$$

The constrained equilibrium could, for example, consist of returning to the vapor the last incoming molecule to form an (n_m+1) cluster. Such a constraint is equivalent to the introduction of a perfectly reflecting boundary at n_m+1 in the set of master equations. The derivation of Eq. (19) also assumed that only single step processes occurred, i.e., that clusters could only gain or lose one molecule at a time. Detailed balance was used in the conventional manner to obtain Eq. (19) in order to relate the evaporation coefficients γ to the condensation coefficients β. One can point out that if the evaporation and condensation coefficients are known, one can also solve directly the set of master equations (1a) and (1b) without making use of detailed balance. By assuming a sticking coefficient equal to unity, β in the CNT is related to the pressure P by $\beta(n,n+1)=Pa_n/\sqrt{2\pi mkT}$. The gas being assumed ideal, P is given by $(N-n)kT/(V-nv)$. It follows that

$$\beta(n,n+1)=\frac{(N-n)}{(V-nv)}\sqrt{\frac{kT}{2\pi m}}a_n, \tag{21}$$

where m is the mass of a molecule.

IV. SIMULATION USING MOLECULAR DYNAMICS

Having appealed to CNT to elaborate many of the semiquantitative features of homogeneous nucleation in a small system, we now turn to the quantitative study of the same system by means of MD. Again, we focus on homogeneous nucleation in argon vapor and for the intermolecular potential $u(r)$, where r is the distance between two argon atoms, we use the Lennard-Jones (LJ) form

$$u(r)=4u_0\left[\left(\frac{r_0}{r}\right)^{12}-\left(\frac{r_0}{r}\right)^{6}\right] \tag{22}$$

with $u_0/kT=119.8/T$ and $r_0=0.3405$ nm.[29] The temperature is fixed at 85 K throughout the present study. The potential energy of the system as a whole is assumed to be pairwise additive.

In the following, distances are expressed in units of r_0 and energies in units of kT. Furthermore mass is expressed in units of m the mass of a single argon atom. It follows that the units of force, acceleration, velocity, and time are, respectively, kT/r_0, kT/mr_0, $\sqrt{kT/m}$, and $r_0\sqrt{m/kT}$ (see also Table I).

The simulation cell, subject to periodic boundary conditions, is chosen as a cubic box of side length c and the tail of the LJ potential is cut off at $r=r_c=c/2$. In the present study, the cell contains $N=216$ argon atoms. These are initially distributed on a simple cubic lattice of lattice parameter $c/6$, so that the atoms closest to the cell faces are at a distance $c/12$ from those faces. In order to have a reasonably random initial configuration, the three coordinates of each atom were then modified by the addition of a random number lying in the interval $[-(c/6-1)/2,+(c/6-1)/2]$. Initially, each atom is assigned three velocity components v_x, v_y, v_z, drawn from a normal curve of zero mean and unit standard deviation. This corresponds to the usual Maxwell–Boltzmann (MB) velocity distribution[30] at temperature T, provided that $\sqrt{kT/m}$ is used as the unit of velocity, as mentioned above. The mean dimensionless kinetic energy of an atom is therefore equal to 1.5.

TABLE I. Units used in the simulation, and their numerical values. Note that the units of force, acceleration, velocity, and time are consequences of the choice of the length, energy, and mass units.

	Unit	Value in SI units
Length	r_0	3.405×10^{-10} m
Energy	kT	1.1736×10^{-21} J
Mass	m	6.6336×10^{-26} kg
Force	$\frac{kT}{r_0}$	3.4466×10^{-12} N
Acceleration	$\frac{kT}{mr_0}$	5.1957×10^{13} m s^{-2}
Velocity	$\sqrt{\frac{kT}{m}}$	1.3301×10^{2} m s^{-1}
Time	$r_0\sqrt{\frac{m}{kT}}$	2.5600×10^{-12} s

To move the atoms, the ''velocity-Verlet'' algorithm was used,[31,32] care being taken to account for the periodic boundary conditions as well as for the formation of a cluster. The coordinate $x(t+\Delta t)$ is given as a function of the coordinate $x(t)$, velocity $v_x(t)$, and acceleration $a_x(t)$ at time t, while the velocity component $v_x(t+\Delta t)$ is updated using $v_x(t)$, $a_x(t)$, and $a_x(t+\Delta t)$:

$$x(t+\Delta t)=x(t)+v_x(t)\Delta t+\tfrac{1}{2}a_x(t)(\Delta t)^2, \tag{23a}$$

$$v_x(t+\Delta t)=v_x(t)+\tfrac{1}{2}[a_x(t)+a_x(t+\Delta t)]\Delta t. \tag{23b}$$

Analogous expressions apply to the y and z coordinates and to the corresponding velocity components. Clusters were defined as ''Stillinger clusters''[22] with a ''connectivity distance'' $d_c=1.5$. There is evidence that a finite variation of d_c in the neighborhood of 1.5 does not lead to a significant change in the cluster equilibrium size distribution.[4,9,12] Among other things, this definition does not allow an atom to belong to more than one cluster. At any given time, many clusters exist in the cell, especially if an isolated atom is viewed as a cluster. However, we adopt the rule that only the largest cluster (say size n) in the cell (under the Stillinger definition) is to be regarded as *the cluster*. Smaller entities that satisfy the Stillinger definition are considered to be part of the surrounding vapor. We used the method of Sevick *et al.*[33] to identify the atoms composing the largest cluster in

the cell. Once these atoms are listed, the center of mass of the corresponding cluster is computed, and the cluster, along with the vapor atoms, is translated rigidly to bring the center of mass to the center of the cell. Periodic boundary conditions are preserved during this translation in which n_w vapor atoms may be moved out of the cell and reintroduced as periodic images through an opposite wall. All atoms of the central cell are then replicated in the 26 neighboring cells.

Although several options exist for maintaining the temperature of the system, we chose the following. After shifting the center of mass to the center of the cell, n_w atoms are randomly selected among the $N-n$ nonconnected atoms and their velocity components are assigned new values, randomly reselected from the MB distribution, and subject only to the constraint that their kinetic energies must be, on the average, equal to 1.5, i.e., the average in the initial state. Evidently, this method causes the temperature of the system to fluctuate considerably as the simulation proceeds, because the number n_w of escaping atoms varies appreciably from step to step. However, this procedure has the advantage of not introducing an arbitrary rate at which vapor atoms are heated or cooled. Furthermore, the method imitates, fairly well, the energy distribution of the atoms surrounding a cluster in a macroscopic system. Another possibility would involve reselecting the velocity components of all the $N-n$ nonclustered atoms after each time step. This would maintain the temperature of the gas fixed and would more closely resemble the situation in the presence of a carrier gas even if that gas affected the energy of the cluster itself.

It may be noticed that this heat bath looks like an ''Andersen thermostat.''[34] The difference with this method is that we do not choose arbitrarily the frequency of the stochastic collisions with the virtual molecules of the heat bath. In contrast, we rescale the velocity of a number of nonconnected atoms (i.e., reascribe them as MB velocities), this number being defined by the system itself. This number is equal to the number of atoms leaving the cell per time step. One can point out that we thus proceed by small constant-energy pieces, because between two rescaling procedures, we solve the Newtonian laws of motion that preserve the energy. However, over a long simulation, the system behaves as an (N,V,T) system because it is actually in contact with a heat bath which avoids a temperature drift. So, as in the case of the Andersen thermostat, our method is compatible with a canonical simulation.[34] On the other hand, the dynamical properties of the system do indeed depend on the thermostating method. This is, however, not our concern here because we are focusing on intrinsic properties of the cluster formed within the metastable argon vapor.

In addition, we may stress that the evaporation and condensation coefficients γ and β are determined as a function of the size of the cluster and of its kinetic temperature. So, even though our constant-temperature simulation may display more fluctuations than would other thermostating methods (e.g., the Nosé–Hoover thermostat),[34] this is not a serious drawback in the present context. The only point is that another thermostat leads to smaller fluctuations of the cluster temperature, the γ's and β's are better defined (less statistical noise), because the required temperature appears more frequently during a given simulation time.

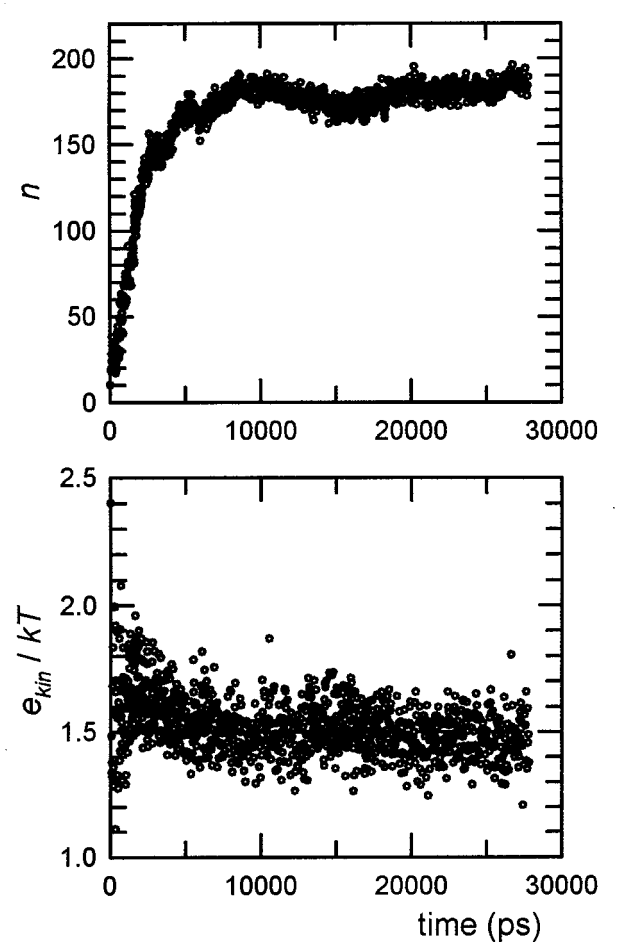

FIG. 4. MD time evolution of cluster size n for $N=216$ in a container of volume $V/r_0^3=6000$ ($r_0=0.3405$ nm) corresponding to an initial degree of supersaturation of ≈ 13.75 (top frame). Evolution of the mean kinetic energy per cluster molecule, over same time interval (bottom frame).

Although there may be more efficient methods for thermostating the system, it is important to note, in the following, that the system does come to thermal equilibrium. The evidence for this is reasonably clear in Fig. 4 where the effect of the latent heat of condensation is demonstrated. At first, the average kinetic energy of the cluster is high (the cluster is heated by the condensation). As time passes, the temperature of the cluster decreases to the thermal equilibrium value. That thermal equilibrium is achieved is also demonstrated by the development of the large equilibrium cluster represented by the large peak in Fig. 5. Furthermore, this cluster satisfies detailed balance as the concurrence of the filled and open circles indicates. Further indication of the satisfaction of the principle of detailed balance is of course presented in Fig. 6. With other methods of thermostating, it might not have been possible to display the effect of the latent heat, as in Fig. 4.

V. SIMULATION RESULTS

A. Small systems at equilibrium

Typical time evolutions of cluster size and mean cluster kinetic energy per cluster atom are plotted in Fig. 4, for an

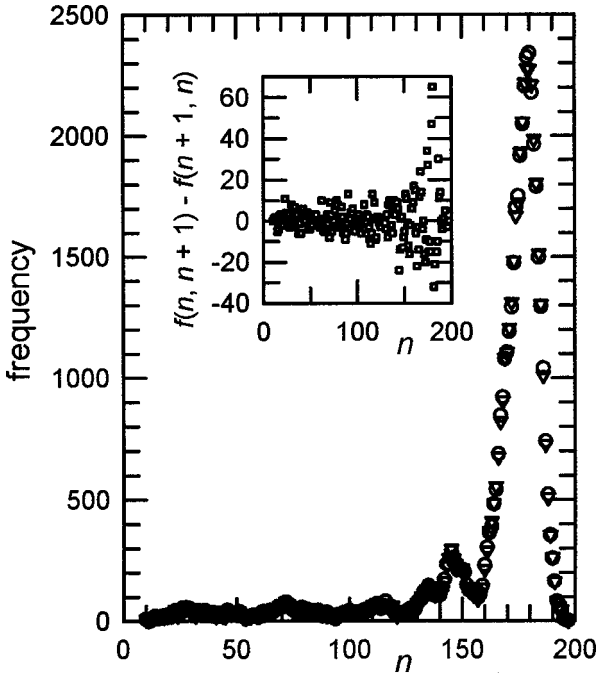

FIG. 5. Illustration of validity of detailed balance. In the simulation in Fig. 4, all $n \rightarrow n+1$ and $n+1 \rightarrow n$ transitions were enumerated. The corresponding frequencies of occurrence $f(n,n+1)$ (circles) and $f(n+1,n)$ (triangles) exhibit good agreement with the detailed balance expectation for all cluster sizes n, even for the smallest clusters that do not correspond to equilibrium. This is emphasized by the inset where the frequency difference is plotted as a function of n.

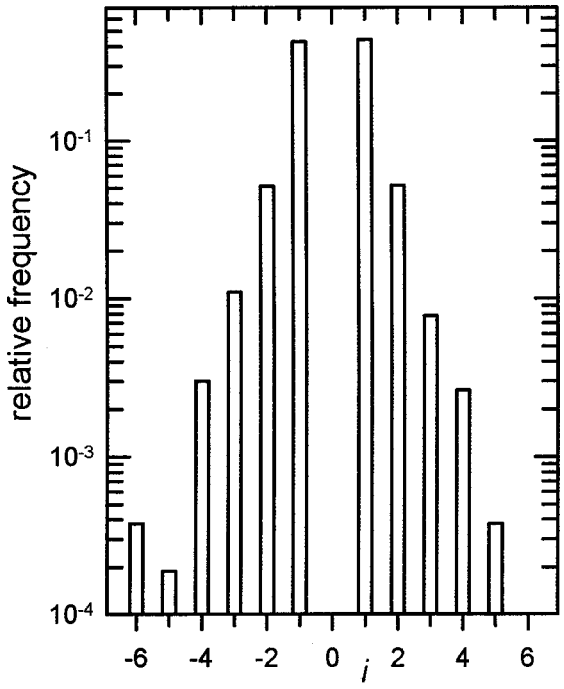

FIG. 6. Relative frequencies of $n \rightarrow n+i$ and $n \rightarrow n-i$ transitions near the mean size ($n=180$) of the equilibrium cluster (see Fig. 7). Frequencies are again from the simulation in Fig. 4 (total number of events=5299). The symmetry in the histogram confirms, as expected from detailed balance, that evaporation and condensation are equally probable for a cluster in equilibrium.

initial supersaturation of ≈ 13.75, assuming that the vapor behaves ideally. For such a system, CNT adapted to small systems, yields a critical nucleus with $n^* \approx 7$, if the surface tension is taken to be 13.2 mJ m^{-2}. Thus, the simulation cannot show this small nucleus, but only the growth of a cluster that is stabilized at an equilibrium value of n of the order of 180 molecules. Notice that CNT, adapted to small systems, has played a useful role *vis à vis* the simulation by alerting us to the fact that we should probably not be able to observe any irregularity signifying the appearance of the critical nucleus.

The mean kinetic energy per cluster atom, also plotted in Fig. 4, is larger than 1.5 kT during the growth stage (as would be expected due to the latent heat of condensation), but it stabilizes at about 1.5 kT once the cluster reaches its equilibrium size. However, in this final state there are, as expected, large and long term energy fluctuations.

Once equilibrium is reached, it is possible to determine the frequencies at which size transitions occur involving the loss or addition of various multiplets of molecules. We begin by noting that in an MD simulation one can, at the end of every time step δt (10 fs in the present work) determine the status of the cluster, i.e., determine the number of cluster molecules (atoms) that constitute the cluster. Comparing this number with the number determined after the preceding step immediately reveals whether the cluster has lost (by evaporation) or gained (by condensation) one or several molecules, or whether it maintained its original size during the time step. Note that, in the latter case, we would not know whether the cluster had actually not lost or gained molecules or whether losses and gains had canceled one another. As a matter of fact, however, this sort of exact compensation within a single time step is highly unlikely, as we show below.

Figure 5 shows a typical example for the frequencies of the $n \rightarrow n+1$ and $n+1 \rightarrow n$ transitions. The identity of both frequency distributions confirms the validity of detailed balance. Figure 6 shows the frequencies measured for $n \rightarrow n \pm i$ transitions. It can be seen that, for this system, $n \rightarrow n \pm 2$ and $n \rightarrow n \pm 3$ transitions account, respectively, for about 10 and 2% of all transitions. Higher order events are negligible. The almost perfect symmetry of the histogram, in Fig. 6 again confirms the validity of detailed balance. It should, however, be mentioned that the histogram cannot be rigorously symmetric due to the small size of the system. It would have been totally symmetric if the histogram of the transitions $n \rightarrow n+i$ and $n+i \rightarrow n$ had been plotted.

Figure 6 also shows that multiple step transitions are important, and confirms, by an independent means, the earlier observation of ten Wolde *et al.*[35] who used linear response theory to demonstrate this fact.

In Fig. 7 we compare the cluster size distributions obtained via MD with those obtained via CNT, i.e., through the application of Eqs. (15) and (16). The comparison was made for several initial supersaturations S_{init}. In each case, the location of the maximum of the theoretical (CNT) distribution was adjusted to the maximum of the simulated distribution by varying the surface tension used in the CNT. It emerges that values of σ in the neighborhood of 14 mJ m^{-2} are required. These values are close to the experimental

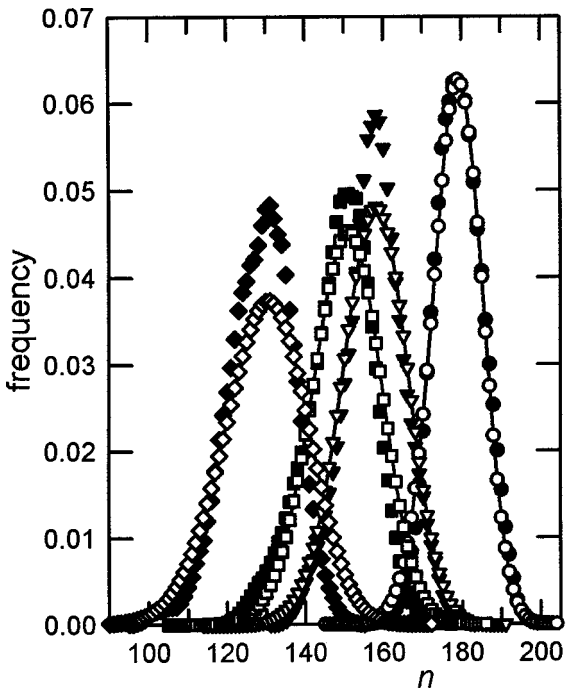

FIG. 7. Comparison of the fluctuation in size of an ''equilibrium cluster,'' corresponding to different container volumes, (i) via MD simulation (closed symbols) and (ii) via CNT, Eqs. (15) and (16) (open symbols). $N=216$ and $V/r_0^3=6000$ (circles), 8000 (triangles), 10 000 (squares), 12 000 (diamonds). Surface tension σ has been used as an adjustable parameter to bring the abscissa of the maximum of the CNT fluctuation curves into coincidence with their simulated counterparts : $\sigma=13.9$, 15.5, 13.6, and 14.1 mJ m^{-2}, respectively, from $V/r_0^3=6000$ up to 12 000. The areas under all distributions are normalized to unity.

value[36] of 13.2 mJ m^{-2}. Simulated values of the surface tension[37] lie a bit higher than the experimental value and a consensus has developed that in comparing CNT with the results of simulation, one should use the simulated value of surface tension in CNT.[10]

Nevertheless, it is obvious from this comparison that the small system CNT provides a reasonable first approximation to the distribution obtained via computer experiment, and that the approximation is better when the cluster is larger. Thus, once again, the usefulness of the analysis of the small system CNT is demonstrated.

B. Small system kinetics

1. Determination of evaporation coefficients

The evaporation coefficient γ should be more of an intrinsic (internal) property of a cluster than the condensation coefficient β. This follows from the fact that β surely depends on the properties of the surrounding vapor, notably its the pressure. Strictly speaking, however, γ should exhibit a mild dependence on the surrounding vapor, for example, an evaporation event might not be entirely uncorrelated with a condensation event. Just how dependent γ is on the vapor can be determined by comparing MD studies of γ performed (in some way) with the cluster within and outside of the vapor, respectively. The results of such studies are described, among other things, below.

The fact that γ is almost an intrinsic property of the cluster argues for concentrating the effort on the MD measurement of γ rather than β. However, a direct MD measurement of β is also possible as we demonstrate below. The usefulness of the small system is truly emphasized in the determination of the kinetic coefficients. Indeed, it allows us to generate and isolate a single cluster (the equilibrium cluster) of variable size (controlled, among other things, by the initial density of the system), and to measure the rates at which the cluster gains or loses molecules.

Having made these prefactory remarks we turn to an explanation of the MD method that we used for the measurement of γ. We must point out that the determination of the values of γ do not rest on the principle of microscopic reversibility. As we have already indicated, an important point in the determination of the evaporation coefficient for a given transition, e.g., $n\rightarrow n-i(i\geqslant 1)$, is that, if the clusters are kept in the vapor, one has to account for the effects of the other evaporation channels ($n\rightarrow n-j$, $j\geqslant 1$ and $j\neq i$) and of the condensation channels ($n\rightarrow n+j$, $j\geqslant 1$). It is likely that the principal effect of these other channels is an increase of the ''noise'' in the simulation. Therefore, extracting the cluster from the vapor, in order to follow its decay, should not change the problem fundamentally, beyond a reduction of the noise due to the additional decay modes possible to the cluster in the vapor. Note that in the extraction procedure the cluster is removed from the cell and its simulation is continued essentially in vacuum. After an evaporation event, it is returned to the cell at its original size and in the state that prevailed (including the state of the system as a whole) before it was removed. The system is then allowed to develop further in accordance with the MD process.

In the simulation, account must be taken of the fact that the evaporation coefficient depends on the cluster temperature,[13] so that γ is not uniquely determined by n alone, but also by the kinetic energy of the molecules composing the cluster. We therefore write the evaporation coefficient for the $n\rightarrow n-i$ transition as $\gamma(n,n-i,e_{\rm kin})$ where $e_{\rm kin}$ is the mean kinetic energy of the cluster atoms.

Once equilibrium and the corresponding cluster of size n is established in the small system, $N(n,n-i,e_{\rm kin})$ the number of evaporation events leading from the size n to the size $n-i$ is counted, and t_n the cumulative time, during the simulation, that the cluster spends at size n, regardless of the transitions that take it out of that size, is measured. The evaporation coefficient is then determined from the relation

$$\gamma(n,n-i,e_{\rm kin})t_n=N(n,n-i,e_{\rm kin}). \tag{24}$$

This relation is easily understood, since $\gamma(n,n-i,e_{\rm kin})$ is the probability per unit time that the cluster undergoes transition (fraction of ensemble members that undergo transition in unit time) and t_n is the total time available for it to make a transition.

Note that $N(n,n-i,e_{\rm kin})$ would be zero if $e_{\rm kin}$ were strictly specified, so that we have to work with n clusters whose kinetic energies per atom are located in a narrow interval $e_{\rm kin}\pm\Delta e_{\rm kin}$ (e.g., 1.5 ± 0.005 kT). Care must be exercised in the evaluation of t_n. If the clusters are kept within the vapor, t_n is indeed the sum of the lifetimes of all the n

clusters with energy e_{kin} that appeared during the entire simulation. If the clusters are temporarily withdrawn from the box (cell) so as to be able to follow their decays in the absence of competing condensation processes, t_n is defined similarly, but it then represents the cumulative lifetime of the clusters observed exclusively outside of the box.

The sum of all the events contributing to the cumulative lifetime t_n is $\Sigma_{j\geqslant 1}N(n,n\pm j,e_{\mathrm{kin}})$, so the average lifetime of the n cluster is

$$\langle \tau(n,e_{\mathrm{kin}})\rangle = \frac{t_n}{\Sigma_{j\geqslant 1}N(n,n\pm j,e_{\mathrm{kin}})}. \tag{25}$$

Notice that this quantity is the average lifetime of an n cluster regardless of the number j of molecules lost or gained in a single transition. This average lifetime is necessarily shorter than the reciprocal of $\gamma(n,n-i,e_{\mathrm{kin}})$ since it is a lifetime terminated by any one of several possible transitions rather than by the transition $n\rightarrow n-i$, alone. Substitution of Eq. (25) into Eq. (24) yields

$$\gamma(n,n-i,e_{\mathrm{kin}}) = \frac{1}{\langle \tau(n,e_{\mathrm{kin}})\rangle}\frac{N(n,n-i,e_{\mathrm{kin}})}{\Sigma_{j\geqslant 1}N(n,n\pm j,e_{\mathrm{kin}})}. \tag{26}$$

This shows that $\gamma(n,n-i,e_{\mathrm{kin}})$ is simply the reciprocal of the overall average lifetime $\langle \tau(n,e_{\mathrm{kin}})\rangle$ weighted by the relative frequency of the $n\rightarrow n-i$ transition under consideration. In Eq. (26), it has been assumed that the different types of evaporation and condensation processes are independent and uncorrelated.

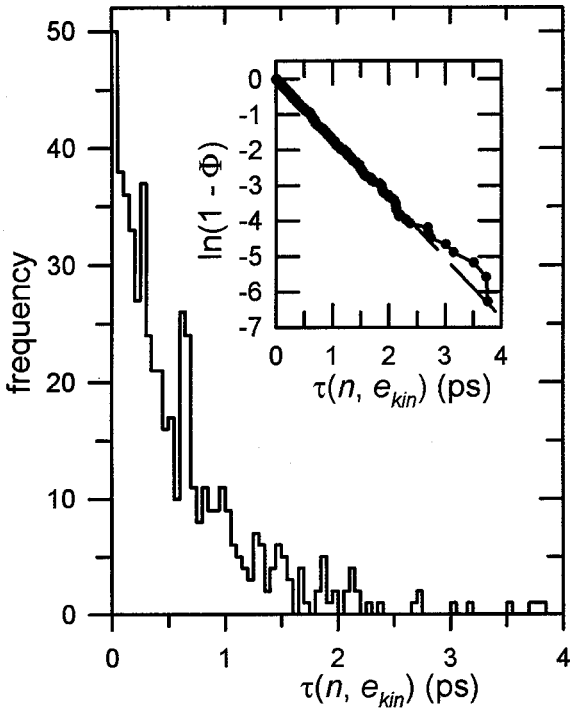

FIG. 8. Distribution of the lifetimes of n clusters ($n=150$) prepared in a container with $V/r_0^3=10\,000$. The selected clusters have kinetic energies per cluster molecule lying between 1.495 and 1.505 units of kT. The linear dependence of ln(1-Φ) (dashed line) on lifetime τ shows that τ has an exponential dependence on kinetic energy (Φ is the normalized cumulative frequency).

2. Refinements and applications

Observation of the lifetimes shows that, even for a given n, they fluctuate from one n cluster to another. This is due, on the one hand, to the fluctuation of the kinetic energy of the cluster molecules and, on the other hand, to the fact that the lifetime is a random variable. An example is shown in Fig. 8 where the frequencies of occurrence of the observed lifetimes $\tau(n,e_{\mathrm{kin}})$ are displayed for $n=150$ and for e_{kin} limited by $1.495\leqslant e_{\mathrm{kin}}/kT\leqslant 1.505$. These lifetimes are from a simulation performed in a box of volume $V/r_0^3=10\,000$, and where the lifetimes are determined for clusters removed from the box. It is easy to demonstrate that if a random variable x obeys an exponential law, the logarithm of $1-\Phi(x)$, where $\Phi(x)$ is the normalized cumulative frequency of x, is a linear function of x. The inset in Fig. 8 demonstrates that this linear dependence is actually observed for $\tau(n,e_{\mathrm{kin}})$ (see the dashed line fitted to data points out to $\tau(n,e_{\mathrm{kin}})=2$ ps, i.e., taking only lifetimes for which the observed frequencies appear to be reliable). This linearity proves that the probability that the cluster has not undergone a transition decays exponentially with time, i.e., that the decay is a first order process like radioactive decay. It is worth mentioning that this result also proves that the evolution of cluster size can be described by the set of linear master equations, Eq. (1).

Use of one of the equivalent relations, Eq. (24) or (26), yields $\gamma(n,n-i,e_{\mathrm{kin}})$, but using n clusters in only one chosen narrow interval $e_{\mathrm{kin}}\pm\Delta e_{\mathrm{kin}}$ constitutes a waste of information and, as a consequence, an unduly large uncertainty in the measured evaporation coefficient. To reduce the scatter of the data for this parameter, it can be determined for a series of intervals centered on values of e_{kin} and spaced by $2\Delta e_{\mathrm{kin}}$. Following Zhukhovitskii,[13] we have assumed that γ depends exponentially on the kinetic energy of the cluster molecules, even though this is not rigorous, at least for small systems.[38] Therefore, $\ln\gamma(n,n-i,e_{\mathrm{kin}})$ should be a linear function of e_{kin} and the experimental γ's can be fitted to a straight line (see an example in Fig. 9). Thus we write

$$y(n,n-i,e_{\mathrm{kin}}) = \ln\gamma(n,n-1,e_{\mathrm{kin}}) = a_0 + a_1 e_{\mathrm{kin}}, \tag{27}$$

where a_0 and a_1 are the free parameters of a least squares fit. The dependence of a_0 and a_1 on n is exhibited in the inset of Fig. 9. The data are taken from a simulation performed in a box of volume $V/r_0^3=10\,000$ where clusters were temporarily withdrawn from the box for the determination of lifetimes.

With a_0 and a_1 in hand, it is possible to compute $y(n,n-i,e_{\mathrm{kin}})$ for any value of e_{kin}, and especially for 1.5 kT which corresponds to $T=85$ K, the temperature of the heat bath in our simulations. One can also determine the 95% prediction interval from the linear regression, Eq. (27) and arrive at an estimate of the uncertainty $\Delta y(n,n-i,e_{\mathrm{kin}})$ in $y(n,n-i,e_{\mathrm{kin}})$. Finally, one arrives at the desired evaporation coefficient

$$\gamma(n,n-i,e_{\mathrm{kin}})\pm\Delta\gamma(n,n-i,e_{\mathrm{kin}}) = \exp[y(n,n-i,e_{\mathrm{kin}}\pm\Delta y(n,n-i,e_{\mathrm{kin}})]. \tag{28}$$

The general procedure described above has been used to evaluate $\gamma(n,n-i,1.5\,kT)$ from the raw data derived from

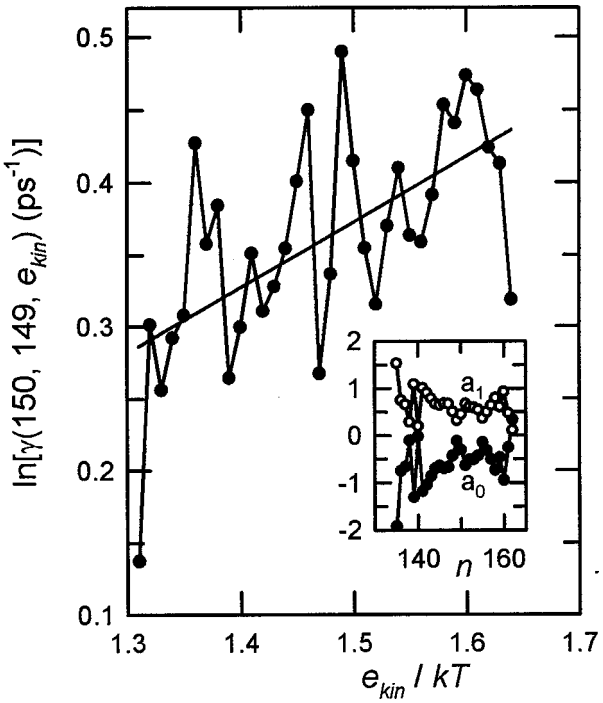

FIG. 9. Dependence of the logarithm of the evaporation coefficient $\gamma(n,n-1,e_{\mathrm{kin}})$, for $n=150$, on temperature measured as e_{kin}. γ is determined outside of the container. The dependence on n of the coefficients a_0 and a_1 [Eq. (27)], determined via a least squares fit, is exhibited in the inset.

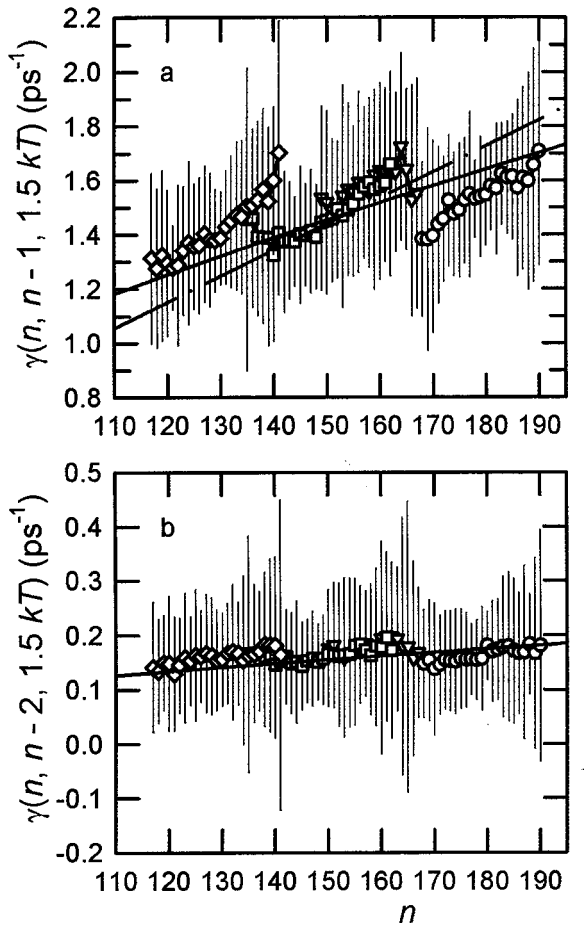

FIG. 10. Dependence on n of evaporation coefficients for the transitions, (a) $n\rightarrow n-1$ and (b) $n\rightarrow n-2$, with $e_{\mathrm{kin}}=1.5\,kT$. The coefficients were determined by the method illustrated in Fig. 9. The four symbols correspond to $V/r_0^3=6000$ (circles), 8000 (triangles), 10 000 (squares), 12 000 (diamonds). Error bars indicate 95% prediction intervals. Solid and dashed–dotted lines represent, respectively, $n^{2/3}$ and n dependence of γ on n.

the MD simulation for four box volumes, $V/r_0^3=6000$, 8000, 10 000, and 12 000 [Figs. 10(a) and 10(b)]. Note that lifetimes observed outside of the box were used. It is clear that the general trend is for γ to increase with n. However, the scatter of the results [especially in Fig. 10(a)] is such that it is difficult to draw the conclusion that γ actually follows the $n^{2/3}$ law (displayed as a dashed–dotted line drawn somewhat arbitrarily in the figure) expected for a cluster that resembles a spherical drop. The simplest hypothesis for this scatter is that the simulations should have been much longer in order to generate larger numbers of clusters of a given size. Also, it is desirable to perform simulations with boxes having other volumes. Indeed, Figs 10(a) and 10(b) suggests that each of the four volumes yields a series of γ's which does not (or at least not systematically) overlap the other series. This seems to indicate that these determinations are somehow box-dependent (even though the clusters were temporarily withdrawn from the box for the determination of their lifetimes) and would suggest that they be carried out in boxes of still larger volume where subtle boundary effects (in spite of the use of periodic boundary conditions) would be less influential. Also, recall that the ''cutoff distance'' r_c for the LJ potential was chosen to be $c/2$, so that (to some degree) the potential was a function of the box.

In addition, the observed increase of γ with increasing n seems to obey a linear law (solid line) better than an $n^{2/3}$ law. This suggests that the clusters are too small (or not very compact) to have a sharply discontinuous surface and a uniform core. In other words, even molecules located ''inside'' the cluster are able to escape with a probability not much smaller than those in the ''envelope'' of the cluster, with the consequence that γ is roughly proportional to n, and not to $n^{2/3}$.

For the sake of completeness, we show in Figs. 11(a) and 11(b), a comparison of evaporation coefficients, as a function of n, obtained by removing clusters from the box with coefficients obtained, keeping the clusters in the box. Both sets of data were simulated, by the method described above, with the mean kinetic energy of the cluster fixed at 1.5 kT. Data for (a) the $n\rightarrow n-1$ transition and (b) the $n\rightarrow n-2$ transition are used. The open circles refer to clusters kept in the vapor while the filled circles refer to those that were removed. The volume of the box was $V/r_0^3=10\,000$. As it can be seen the agreement between the two series of γ is very good, confirming that, within the accuracy of our simulations, γ can be determined indifferently either within the vapor or outside of it. This implies that again, within the accuracy of the simulation, the evaporation coefficient is an intrinsic property of the cluster (unlike the condensation coefficient). It may also be seen that the data is a bit more noisy for the simulations that kept the cluster in the vapor, in agreement with our expectations, mentioned earlier.

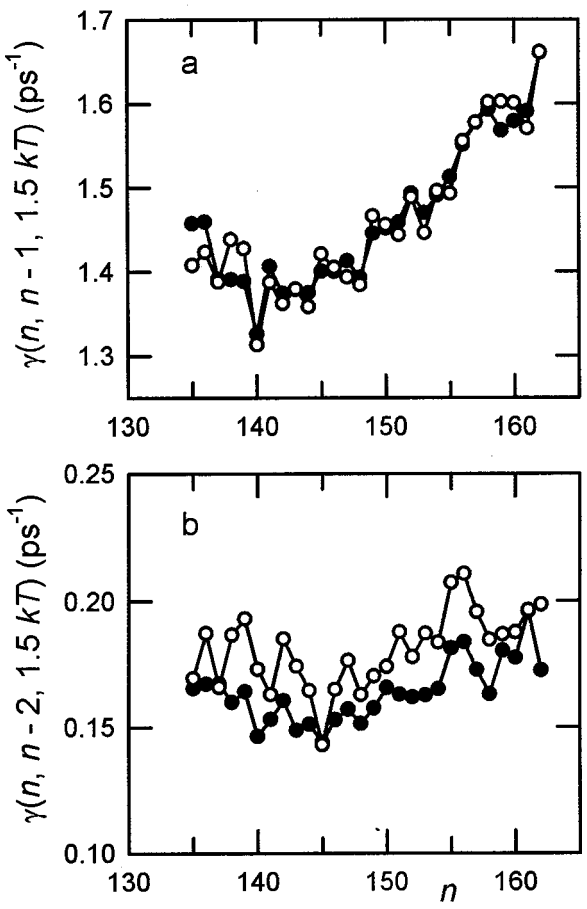

FIG. 11. Comparison of the values of evaporation coefficients as determined outside the container (solid circles) and inside the container (open circles), respectively. (a) $n \rightarrow n-1$ transitions, (b) $n \rightarrow n-2$ transitions. $e_{\mathrm{kin}} = 1.5\,kT$.

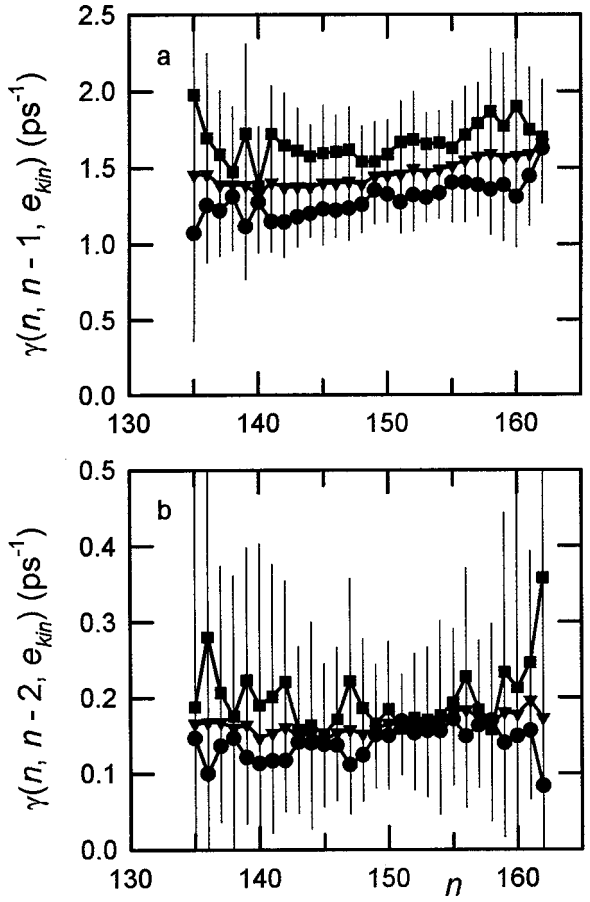

FIG. 12. Effect of the temperature (or cluster kinetic energy) on the evaporation coefficient for (a) the $n \rightarrow n-1$ transitions and (b) the $n \rightarrow n-2$ transitions; $e_{\mathrm{kin}} = 1.3\,kT$ (disks), $1.5\,kT$ (triangles), $1.7\,kT$ (squares).

In addition, Fig. 12 shows the values of γ for (a) the $n \rightarrow n-1$ and (b) the $n \rightarrow n-2$ transitions, for three different temperatures. In spite of the noise, it is clear that $\gamma(n, n-1, e_{\mathrm{kin}})$ increases systematically with temperature; on the average, at 1.7 kT, γ is roughly 14% higher than at 1.5 kT and 30% higher than at 1.3 kT. The same trend is observed for $\gamma(n, n-2, e_{\mathrm{kin}})$, although it is less obvious due to the scatter of the results.

VI. MULTIMOLECULE EVENTS INVOLVE CLUSTERS. EVALUATION OF β

γ in Fig. 10(a) is of the order of 1–2 ps^{-1}. The average number of molecules ejected within a 10 fs time step is therefore of the order of 0.01–0.02. Assuming that the number of ejected molecules is a random variable distributed according to Poisson's law, leads to the conclusion that the uncorrelated ejection of two molecules within 10 fs is at least 100 times less probable than the ejection of a single molecule. This supports the hypothesis that, in most of the observed multimolecule events, the ejected molecules are clusters. The same reasoning, based on Poisson's law, leads to the conclusion that the simultaneous (same time step) arrival of a single molecule and the departure of another is also a rare event.

Using a procedure similar to that described in Secs. V B 1 and V B 2 for the determination of γ, we have also evaluated the condensation coefficients $\beta(n-i, n, e_{\mathrm{kin}})$ directly from the simulations, independently from the determination of γ and thus by making neither use of the values of γ, nor by using the principle of detailed balance. It should be noted that the definition of these β's is consistent with the condensation coefficients appearing in the set of master equations, Eq. (1). The coefficients are related to the rate of arrival and to the sticking probabilities of molecules in the surrounding vapor. In Fig. 13, we show the evaporation coefficients taken from Fig. 11(a), as well as the condensation coefficients $\beta(n-1, n, e_{\mathrm{kin}})$, necessarily determined *in* the box, at $e_{\mathrm{kin}} = 1.5\,kT$. It is interesting to see that β and γ have the same value at $n \approx 150$, i.e., at the mean size of the equilibrium cluster as it should be (see Fig. 7).

It is possible to compare this ''experimental'' estimate of β with that derived from the simple kinetic argument expressed by Eq. (21). For example, for a cluster of size 150, the value of ≈ 1.45 ps^{-1} (Fig. 12) is roughly one order of magnitude larger than the value ≈ 0.16 ps^{-1} of β predicted by Eq. (21). This can be explained by a large increase of the cross section for capture of molecules from the vapor due to the diffuse nature of the outer layer of the cluster and also as a result of its attractive potential.[39–41] This result re-

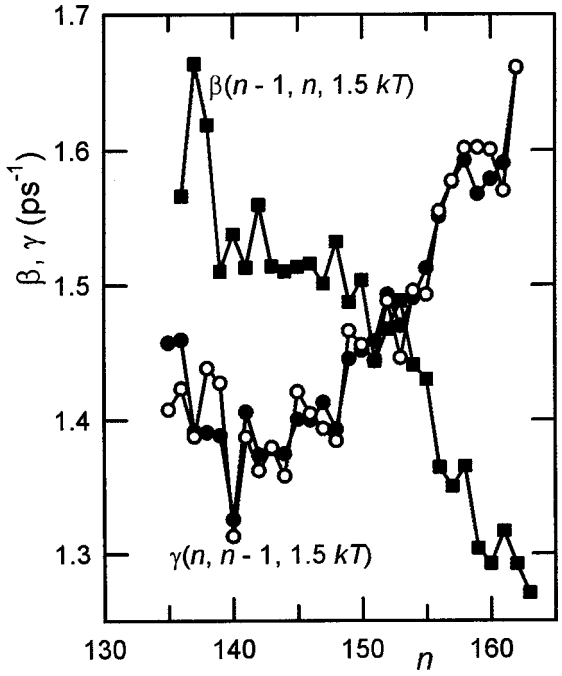

FIG. 13. Dependencies on n of $\gamma(n,n-1,1.5\,kT)$ [same data as in Fig. 11(a)] and $\beta(n-1,n,1.5\,kT)$. The definition of the β's is consistent with the condensation coefficients appearing in the set of master equations, Eq. (1). Note the satisfactory equality of β and γ in the neighborhood of the mean size, $\approx$150, of the equilibrium cluster.

emphasizes the fact that one should not expect an $n^{2/3}$ law for the γ's, but rather a linear increase of magnitude with n.

VII. CONCLUDING REMARKS

We have studied the behavior of a system consisting of a small number of argon molecules (216) in a small volume. The system is initially supersaturated and evolves in time to produce a single *defined* cluster, as it attains equilibrium. The intermediate kinetic process is a ''condensation'' that is observed via a molecular dynamics simulation. The size of the equilibrium cluster that forms fluctuates about a mean (150 molecules) and MD also allows us to observe these fluctuations. We have also characterized the equilibrium cluster by the application of classical nucleation theory (CNT) to the small system, and have found that CNT provides a reasonable semiquantitative account of the more exact behavior of the cluster observed by means of MD.

The underlying thrust of our approach is based on the belief that, with sufficient care, the phenomena in the small system can be ''mapped'' onto a macroscopic system in the thermodynamic limit. This is not a new idea and has been used in a number of simulations of nucleation phenomena.[3,7,8,11,13] In our case, however, the major focus has been on the evaluation of the evaporation and condensation coefficients of molecules leaving and entering a cluster, since general formal theories, based on master equations, exist[42,43] for the nucleation rate, but these equations can only be engaged when the magnitudes of the evaporation and condensation coefficients are substituted in them.

In our case, the ''mapping'' rational is based on the idea that the evaporation coefficient is, to a high degree of approximation, intrinsic to the cluster, i.e., it is essentially independent of whether the cluster is in a small or large system and also independent of the surrounding vapor. From the evaporation coefficients it is possible to derive the magnitude of the condensation coefficients, provided that detailed balance is satisfied. Our simulations have shown, at least for the equilibrium cluster, that this is the case.

Besides yielding the values of the evaporation and condensation coefficients and demonstrating the intrinsic nature of the former, as well as establishing the validity, within the simulation, of detailed balance, our study has demonstrated the importance of multimolecular losses and gains of molecules and the fact that clusters disappear via a first order decay law, thus establishing the relevance of the linear form of the set of master equations that can be used to describe the nucleation rate. In addition, we have performed an analysis, involving the statistics of correlation, that strongly supports the idea that multimolecule losses and gains experienced by a cluster are chiefly due to the departure and arrival of smaller ''clusters.''

Because of the ''intrinsic nature'' of the evaporation coefficient, it is possible to perform the simulations at quite high levels of supersaturation, thereby accelerating the approach to equilibrium, and requiring less computer capacity. The evaporation coefficient of the ''equilibrium cluster'' that forms the object of our measurement is insensitive to the level of supersaturation of the surrounding medium. The condensation coefficient can then be determined by an application of the principle of detailed balance, once the equilibrium distribution of clusters in a particular nucleating system is known.

Our first direct estimates of the condensation coefficients by means of MD indicate that these coefficients are an order of magnitude larger than those predicted by simple molecular kinetic theory, suggesting the effects of the diffuse outer layers of the actual physical cluster and the role of the cluster's attractive potential.

Small systems such as those that we have investigated should be useful as models for the qualitative behavior of large systems *vis à vis* homogeneous nucleation. In this sense they can be used to test the validity of the assumptions entering molecular based theories of the nucleation rate, even though it may not be possible to map all of their features onto a macrosystem.

It should be emphasized that our results represent a ''first effort'' and are still ''noisy'' and preliminary. The present paper is aimed primarily at explaining the method. However, we are optimistic that problems of precision can be largely solved, and it is hoped that other workers will join in the effort.

In closing, for the sake of completeness, and because an admiral study of evaporation coefficients for argon clusters has already been performed by Weerasinghe and Amar[38] using RKK theory[44] and phase space theory (PST),[45] it is appropriate to comment in this paper on the RKK and PST approaches.

Although it is true that these theories represent very important advances, in most cases they are applied to rather rigid molecules with small vibrations and well defined vibra-

tional modes. For example, the application by Weerasinghe and Amar,[38] although to argon clusters, is at low temperatures, e.g., 35 K, far below the triple point of argon at 83.8 K. (It is also confined to quite small clusters.) At these temperatures the cluster is either a rigid glass or a ''magic number'' icosahedron, and well-defined vibrational modes have a meaning. Weerasinghe and Amar make use of this fact in their development. In contrast, in the nucleation problem, we are usually interested in condensation in the neighborhood of the triple point or above. This is the reason that our studies are at 85 K. It is not sure that statistical theories will do much for the problem of *in situ* nucleation of argon at these high temperatures, but as already indicated, they should be mentioned.

As far as phase space theories of rate are concerned, an interesting novel approach that could have far reaching consequences is the ''variational transition state'' approach of Garrett and his co-workers[46] that is still under development. In this approach, the focus is also on evaporation.

We also want to draw special attention to Ref. 10 that describes the temporal development of a cluster, according to MD, in a small system, with the aim of determining the size of the critical nucleus. The authors of this paper were kind enough to supply the present authors with a preprint of their independent work.

ACKNOWLEDGMENTS

This work was partly supported by the French CNRS through an NSF/CNRS travel grant and by the U.S. NSF under Grant No. CHE-0076384 and travel Grant No. NSF INT 9726316. The authors thank Dr. S. Wonczak for stimulating discussions concerning the determination of the evaporation coefficients.

[1] D. J. McGinty, J. Chem. Phys. **58**, 4733 (1973).
[2] J. K. Lee, J. A. Barker, and F. F. Abraham, J. Chem. Phys. **61**, 1221 (1974).
[3] N. G. Garcia and J. M. S. Torroja, Phys. Rev. Lett. **47**, 186 (1981).
[4] M. Rao, B. J. Berne, and M. H. Kalos, J. Chem. Phys. **68**, 1325 (1978).
[5] V. Talanquer and D. W. Oxtoby, J. Chem. Phys. **100**, 5190 (1994).
[6] C. L. Weakliem and H. Reiss, J. Chem. Phys. **99**, 9930 (1993).
[7] P. R. ten Wolde and D. Frenkel, J. Chem. Phys. **109**, 9901 (1998).
[8] K. J. Oh and X. C. Zeng, J. Chem. Phys. **110**, 4471 (1999).
[9] K. Yasuoka and M. Matsumoto, J. Chem. Phys. **109**, 8451 (1998).
[10] K. Laasonen, S. Wonczak, R. Strey, and A. Laaksonen, J. Chem. Phys. **113**, 9741 (2000).
[11] I. Kusaka, Z.-G. Wang, and J. H. Seinfeld, J. Chem. Phys. **108**, 3416 (1998); I. Kusaka and D. W. Oxtoby, *ibid*. **110**, 5249 (1999).
[12] B. Senger, P. Schaaf, D. S. Corti, R. Bowles, J.-C. Voegel, and H. Reiss, J. Chem. Phys. **110**, 6421 (1999); B. Senger, P. Schaaf, D. S. Corti, R. Bowles, D. Pointu, J.-C. Voegel, and H. Reiss, *ibid*. **110**, 6438 (1999).
[13] D. I. Zhukhovitskii, J. Chem. Phys. **103**, 9401 (1995).
[14] R. K. Bowles, J. Chem. Phys. **112**, 1122 (2000).
[15] H. Reiss and R. K. Bowles, J. Chem. Phys. **113**, 8615 (2000).
[16] C. H. Bennett, in *Algorithms for Chemical Computation*, edited by R. E. Christofferson (American Chemical Society, Washington, DC, 1977).
[17] D. Chandler, J. Chem. Phys. **68**, 2959 (1978).
[18] D. Reguera, J. M. Rubí, and A. Pérez-Madrid, J. Chem. Phys. **109**, 5987 (1998).
[19] H. Reiss, W. K. Kegel, and J. L. Katz, J. Phys. Chem. **102**, 8548 (1998).
[20] H. Reiss and R. K. Bowles, J. Chem. Phys. **111**, 9965 (1999).
[21] H. Reiss and R. K. Bowles, J. Chem. Phys. **111**, 7501 (1999).
[22] F. H. Stillinger, J. Chem. Phys. **38**, 1486 (1963).
[23] D. W. Oxtoby, J. Phys.: Condens. Matter **4**, 7627 (1992).
[24] H. Reiss and G. J. M. Koper, J. Phys. Chem. **99**, 7837 (1995).
[25] A. J. Yang, J. Chem. Phys. **82**, 2082 (1985).
[26] Y. De Smet, L. Deriemaeker, and R. Finsy, Langmuir **13**, 6884 (1997).
[27] H. Reiss, *Methods of Thermodynamics* (Dover, New York, 1996), pp. 160–163.
[28] *Handbook of Chemistry and Physics*, 50th ed. (CRC Press, Cleveland, 1969), p. D-167.
[29] T. L. Hill, *An Introduction to Statistical Thermodynamics* (Dover, New York, 1986).
[30] G. W. Castellan, *Physical Chemistry* (Addison-Wesley, Reading, MA, 1964), pp. 52–70.
[31] W. C. Swope, H. C. Andersen, P. H. Behrens, and K. R. Wilson, J. Chem. Phys. **76**, 637 (1982).
[32] M. P. Allen and D. J. Tildesley, *Computer Simulation of Liquids* (Oxford Science, Clarendon, Oxford, 1996).
[33] M. E. Sevick, P. A. Monson, and J. M. Otino, J. Chem. Phys. **88**, 1198 (1988).
[34] D. Frenkel and B. Smit, *Understanding Molecular Simulation* (Academic, San Diego, 1996).
[35] P. R. ten Wolde, M. J. Ruiz-Montero, and D. Frenkel, J. Chem. Phys. **110**, 1591 (1999).
[36] *Handbook of Chemistry and Physics*, 50th ed. (CRC, Cleveland, 1969), p. F-31.
[37] M. Mecke, J. Winkelmann, and J. Fischer, J. Chem. Phys. **107**, 9264 (1997).
[38] S. Weerasinghe and F. G. Amar, J. Chem. Phys. **98**, 4967 (1993).
[39] O. V. Vasil'ev and H. Reiss, J. Chem. Phys. **105**, 2946 (1996).
[40] O. V. Vasil'ev and H. Reiss, Phys. Rev. E **54**, 3950 (1996).
[41] V. M. Novikov, O. V. Vasil'ev, and H. Reiss, Phys. Rev. E **55**, 5743 (1997).
[42] D. T. Wu, J. Chem. Phys. **97**, 2644 (1992).
[43] D. T. Wu, J. Chem. Phys. **99**, 1990 (1993).
[44] O. K. Rice and H. C. Ramsperger, J. Am. Chem. Soc. **50**, 617 (1928); L. S. Kassel, J. Phys. Chem. **32**, 225 (1928).
[45] P. Pechukas and J. C. Light, J. Chem. Phys. **42**, 3281 (1965).
[46] G. K. Schenter, S. M. Kathmann, and B. C. Garrett, J. Chem. Phys. **110**, 7951 (1999); S. M. Kathmann, G. K. Schenter, and B. C. Garrett, *ibid*. **111**, 4688 (1999).